Carbon nanotube closed-ring structures

Oded Hod and Eran Rabani
School of Chemistry, The Sackler Faculty of Exact Science, Tel Aviv University, Tel Aviv 69978, Israel

Roi Baer
Institute of Chemistry and Lise Meitner Center for Quantum Chemistry, The Hebrew University of Jerusalem, Jerusalem 91904, Israel
(Received 2 July 2002; revised manuscript received 28 January 2003; published 14 May 2003)

We study the structure and stability of closed-ring carbon nanotubes using a theoretical model based on the Brenner-Tersoff potential. Many metastable structures can be produced. We focus on two methods of generating such structures. In the first, a ring is formed by geometric folding and is then relaxed into minimum energy using a minimizing algorithm. Short tubes do not stay closed. Yet tubes longer than 18 nm are kinetically stable. The other method starts from a straight carbon nanotube and folds it adiabatically into a closed-ring structure. The two methods give strikingly different structures. The structures of the second method are more stable and exhibit two buckles, independent of the nanotube length. This result is in strict contradiction to an elastic shell model. We analyze the results for the failure of the elastic model.

DOI: 10.1103/PhysRevB.67.195408 PACS number(s): 61.46.+w, 73.22.−f, 62.25.+g, 64.70.Nd

I. INTRODUCTION

Since their discovery,[1] carbon nanotubes have been proposed as ideal candidates for the fabrication of nanoelectronic devices due to their unique physical properties. Carbon nanotubes can be either metallic or semiconducting, they have relatively good thermal conductivity, and unusual mechanical strength.[2] These unique properties make them potential building blocks of future small electronic devices.[3–7]

Numerous studies in the past few years have focused on the mechanical properties of single-wall nanotubes (SWNTs),[8–14] and the role of structural deformation on the electronic properties of SWNTs.[14–22] The experimental and theoretical studies indicate that electronic properties, such as the density of states near the Fermi level and/or the conductance of the tubes, are somewhat sensitive to mechanical deformations. These mechanical deformations include bending and twisting the SWNTs, bond rotation defects, and other various types of defects.

Most studies of deformed SWNTs focus on the role of relatively *small* mechanical deformations, which are observed under standard conditions. One exception is the study of Bernholc and collaborators[11,12] who considered relatively large deformations such as twisting and bending a SWNT until a buckle was formed. They developed a continuum elastic theory to treat these different distortions. With properly chosen parameters the continuum elastic shell model provided a remarkable accurate description of these deformations beyond Hooke's law.[12]

More recently, Liu *et al.*[14] have studied the effects of delocalized and localized deformations on the structural and electronic properties of carbon nanotorus using the tight-binding molecular-dynamics method. Nanotoroidal structures based on carbon nanotubes have been studied in the past.[8–10,23] However, in order to stabilize these structures heptagon-pentagon defects were introduced into the hexagonal atomaric structure of the nanotube, resulting in significant changes of the electronic properties. Liu *et al.*[14] were able to systematically study the transition from delocalized-to-localized deformations. One of their major conclusions was that delocalized deformations result in a small reduction of the electrical conductance, while there is a dramatic reduction in the conductance for localized deformations. The study of Liu *et al.*[14] is interesting from an additional perspective, namely, that these closed-ring structures may be used as building blocks of small electromagnetic devices, and their electronic properties are of primary interest for such applications.

There are still several open issues related to the structural and electronic properties of closed-ring carbon nanotubes. For example, what is the *global* minimum-energy configuration of the closed-ring structure? Can a continuum elastic shell model predict the proper structure of these materials? What is the kinetic stability of these materials? In this work we address these issues related to the structural properties of closed-ring carbon nanotubes. In Sec. II we extend the elastic shell model of Yakobson *et al.*[12] to the case of multibuckle formation required when closed-ring structures are formed. The elastic theory provides a scaling law for the number of buckles formed for a given nanotube length (L) and diameter (d). We find that unlike the case studied by Yakobson *et al.* where the continuum shell model provided quantitative results for the formation of a single buckle, it fails in the multibuckle case. To illustrate this, we have used the Tersoff-Brenner potential to describe the interaction between the carbon atoms,[24] and simulated the formation of closed-ring carbon nanotube structures. In Sec. III we discuss two possible ways to generate the closed-ring structures. The two ways lead to very different local minimum-energy configurations. Interestingly, for a large range of nanotube lengths we find that the lowest-energy configuration observed is characterized by only *two*, well localized, buckles, independent of the length of the corresponding nanotube.

In Sec. IV we study the relative stability of the closed-ring structures. It is important to assess the *kinetic stability* of these structures since, as is well known, these structures are less stable thermodynamically compared to the corresponding nanotubes. We find that even at very high temperatures

the structures are very stable on the time scales of molecular-dynamics (MD) and Monte Carlo (MC) simulation techniques. Therefore, we applied the nudged elastic band (NEB) method[25–27] to obtain the minimum-energy paths between different closed-ring configurations, and the barrier for the opening of the rings into the corresponding nanotubes. Conclusion and future directions are given in Sec. V.

II. ELASTIC SHELL MODEL

In this section we generalize the continuum elastic model of Yakobson *et al.*[12] to treat the case of a closed-ring nanotube. This model was first used by Yakobson *et al.* to study the formation of instabilities in carbon nanotubes that were subjected to large deformations. In bending, it was found that the model provides quantitative results for the critical angle in which the tube buckles. Furthermore, the critical curvature estimated from the shell model was in excellent agreement with extensive simulation of SWNTs.[11,12]

When a SWNT is bent to form a nanoring, one expects that the resulting high-energy structure will relax into a closed polygon that is characterized by many buckles.[14] The number of apexes will depend on the length, diameter, and the mechanical properties of the tube. Yakobson *et al.* estimated the critical strain for sideways buckling to be close to that of a simple rod:

$$\epsilon_c = \frac{1}{2}\left(\frac{\pi d}{l}\right)^2, \tag{1}$$

where d is the diameter of the tube (not the ring) and l is the length of the bent section (for tubes that are longer than 10 nm). For shorter tubes the situation is different, and one finds that for achiral nanotubes

$$\epsilon_c = (0.077\ \text{nm}) d^{-1}, \tag{2}$$

independent of the length l. Assuming that the tube buckles when the local strain on a bent tube is

$$\epsilon_c = \frac{1}{2} K_c d, \tag{3}$$

where K_c is the local critical curvature (and is close to that of an axial compression), Yakobson *et al.* found that the critical curvature for buckling is $K_c = \pi^2 d l^{-2}$ for long tubes, and $K_c = (0.155\ \text{nm}) d^{-2}$ for short tubes. The results (for short tubes) were found to be in excellent agreement with simulations on SWNTs of various diameters, helicities, and length.[11]

One can also define a critical angle for buckling, which is the angle between the open ends of the nanotube at the buckling point. This critical angle for buckling is given by $\theta_c = K_c l$. The result for long tubes is $\theta_c = \pi^2 d l^{-1}$, and for short tubes $\theta_c = (0.155\ \text{nm}) l d^{-2}$.

For a closed-ring structure, the local curvature can be approximated by $K = 2\pi L^{-1}$, where L is the total length of the nanotube. Assuming that the local strain on the closed ring does not change significantly when a buckle is formed, and combining Eqs. (1) and (3) we find that the minimum length of a ring section that will allow buckling formation is given by

$$l = \sqrt{\frac{\pi d L}{2}} \tag{4}$$

for long tubes. The number of apexes is given by the ratio $n = L/l$. Inserting Eq. (4) into this expression, we find that the number of apexes for long tubes is approximated by

$$n = \frac{L}{l} = \sqrt{\frac{2L}{\pi d}}. \tag{5}$$

Equation (5) is the main result of this section. It predicts that the number of apexes increases with the square root of the total length of the closed-ring nanotube, and decreases with the square root of the diameter of the tube. In the limit of $L \to \infty$ the number of apexes will also approach infinity, resulting in a perfect ring structure.

III. SIMULATIONS OF CLOSED-RING CARBON NANOTUBE STRUCTURES

In this section we compare structures obtained from atomistic simulations with those predicted from the continuum elastic shell model presented in the previous section. We use the Brenner potential-energy surface to describe the interactions between the carbon atoms.[24] This three-body potential has been used in the past to study structural properties of carbon nanotubes, with excellent agreement between the simulations and experiments for structural deformations in carbon nanotubes.[11,12] As noted in Ref. 11, the *excellent* agreement between the observed and the computed deformed structures confirms the reliability of simulations based on the Brenner potential.

The empirical form of the Brenner potential has been adjusted to fit thermodynamic properties of graphite and diamond, and therefore can describe the formation and/or breakage of carbon-carbon bonds. In the original formulation of the potential, its second derivatives are discontinuous. Therefore, in order to carry out the conjugate gradient (CG) minimization, we have slightly modified the potential such that its derivatives are continuous.

Two different pathways were taken to construct a closed-ring carbon nanotube. The first is based on a geometric construction of a high-energy nanoring configuration, followed by an energy minimization procedure. The other is based on a reversible adiabatic folding of a carbon nanotube until it closes onto itself. The two different pathways of construction lead to different minimum-energy configurations, and their relative structural and kinetic stabilities are discussed in the next section.

A. Optimizing a ring structure

In order to construct a closed-ring nanotube-based structure we geometrically fold a nanotube into a nanoring. This structure obviously is not a minimum-energy configuration. There is an excess tension in the inner radius of the ring due

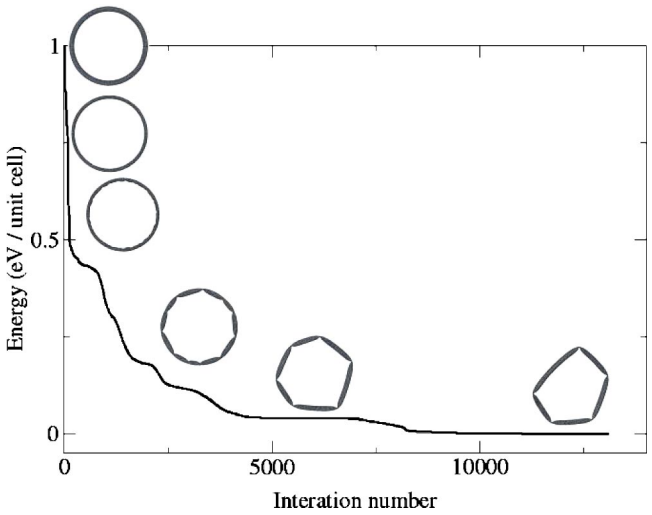

FIG. 1. Conjugate gradient minimization path for a $10\times10\times270$ nanoring. The notation $n\times m\times N$ stands for a $n\times m$ nanotube with N unit-cell length.

to contraction of the carbon-carbon bonds, and there is no compensation from the outer radius where extension of the carbon-carbon bonds occurs. In order to find a local minimum-energy structure of the ring configuration we utilize the CG method applied to the Brenner potential-energy surface.

The results of the CG minimization for a typical nanoring are shown in Fig. 1. The minimization path initially tends to relieve the tension by quenching the inner and outer walls of the ring toward each other, resulting in an increase of the angle distortion energy at the sides of the ring. Apparently this structure is not a local minimum on the potential-energy surface since further application of the CG minimization procedure breaks the cylindrical symmetry of the ring, and produces a polygonal shape, with a large number of apexes. In this structure most of the tension is concentrated in the apexes, while the sides of the polygon resemble that of a normal carbon nanotube. Further minimization results in a reduction of the number of apexes. For most structures studied in this work the CG minimization procedure results in a polygonal structure with a critical angle $\theta_c\approx\pi/3$ for each buckle (see Fig. 2).

We find that below a certain radius of about 2.8 nm ($10\times10\times70$ nanoring) the rings formed using this procedure are unstable. As a consequence of the high initial energy of the carbon nanoring, the CG minimization procedure results in ''melting'' the ring. For higher values of the initial nanoring radius we find that there is a minimum-energy configuration that corresponds to a polygonal structure.

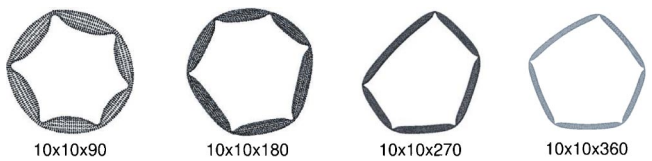

FIG. 2. Polygon structures formed using the geometric construction for different 10×10 nanotube length. Note that the minimization to a polygonal structure is reminiscence of macroscopic behavior, similar to what one finds when folding a straw.

In Fig. 2 we plot several polygonal structures that were formed following the above-outlined minimization procedure. The results obtained for four different tube lengths are shown in the figure: $10\times10\times90$, $10\times10\times180$, $10\times10\times270$, and $10\times10\times360$. The diameter of the nanotube is $d=13.75$ Å, and the length of a unit cell is 2.49 Å. The largest closed-ring structure studied is made of a tube that is ≈0.1-μm long (this is the largest nanotube which formed a polygonal structure using this procedure). As can be seen in Fig. 2 this procedure produces closed-ring structure with five–six buckles. The only systematic behavior observed is that the number of buckles, and thus the number of apexes, are independent of the length of the original nanotube. Similar results were obtained for a series of 5×5 tubes (not shown). However, unlike the case shown in Fig. 2 for a 10×10 tube, the smaller diameter 5×5 tube ($d=6.875$ Å) produced a perfect ring structure for a tube length corresponding to 180 unit cells or larger (see Fig. 5 below). In general we find a strong correlation between the critical length required to form a perfect ring structure and the diameter of the nanotube: nanotubes with smaller diameters will form perfect ring structure for smaller tube lengths. We return to discuss the case of the 5×5 tubes below.

The fact that the number of apexes is independent of the length of the original nanotube (for tube lengths that form polygonal structures) is surprising, since this means that the elastic shell model, which provided quantitative results for the critical strain and critical angle for the formation of a single buckle, fails when multiple buckles are formed. The elastic shell model predicts that the number of apexes grows with the square root of the length of the original nanotube, for long tubes. Furthermore, this model predicts that the critical angle for buckling depends on the length of the apexes. As can be seen in Fig. 2, this is not the case, and the critical angle for buckling is $\theta_c\approx\pi/3$, independent of the tube length. Only above a certain length do we find that the tubes form a perfect ring structure, and at this critical length the buckling disappears. We note in passing that the smaller tubes studied ($10\times10\times90$ and $10\times10\times180$) form six buckles, where the length of each apex is smaller than the threshold required for the continuum theory to hold (10 nm). Below this threshold Yakobson *et al.*[12] found deviations between the elastic shell model and the simulation results even when a single buckle is formed. The deviations were attributed mainly to the fact that the average curvature is less than the local curvature.

B. Reversible adiabatic folding

In contrast to the method outlined in the above subsection, where we started the optimization from a closed ring, we now discuss results that are obtained from adiabatically bending an initially straight tube into a closed-ring structure. This procedure, as will be seen, gives still new structures, not seen in the previous one.

Buckling formation due to critical strain folding was discussed by Brabec and collaborators[11,12] and by Rochefort

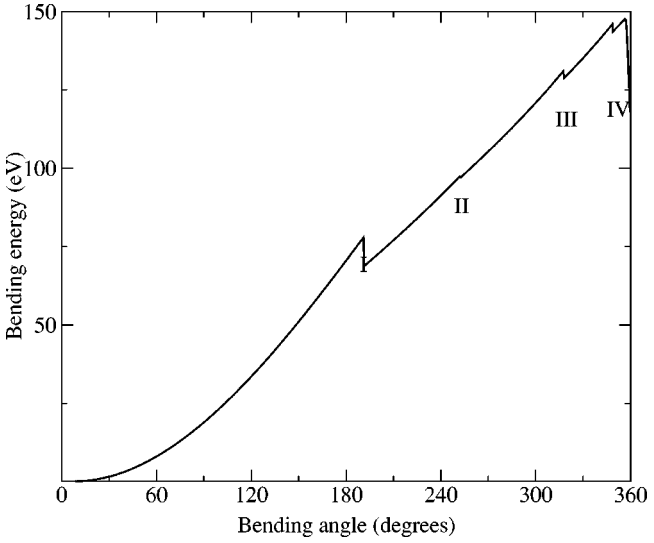

FIG. 3. Total energy versus bending angle for an adiabatic folding of a $5\times5\times45$ nanotube.

et al.[18] These groups reported a parabolic behavior of the energy as a function of bending angle before the buckle formation and a linear behavior thereafter. We have performed similar calculations where the initial carbon nanotube was folded adiabatically into a closed-ring structure. The tube was bent by forcing a torque on the edge atoms stepwise, and after each angle step a full relaxation of the molecular structure under the constraint of fixed edge atom positions was achieved. The results for the total energy versus the bending angle are shown in Fig. 3.

For small angles, the entire nanotube folds without a considerable change in the circular cross section. This result is in agreement with the calculations of Yakobson *et al.*[12] and Rochefort *et al.*[18] For larger bending angles the tube's cross section reduces, and the symmetrically half-circular shape transforms into an ellipse. When the bending angle reaches a critical value *two* kinks are formed and the nanotube buckles as indicated in Figs. 4(a) and 4(b). The first buckling point [i.e., the formation of Fig. 4(b)] corresponds to mark number *I* on the energy diagram shown in Fig. 3. The reason that two kinks are formed while only one kink was formed in the simulation results presented by Yakobson *et al.* is that the tubes studied here are much longer than those studied by Yakobson *et al.* We note in passing that our procedure yielded only one buckle, in agreement with the results reported by Yakobson *et al.* when applied to shorter nanotubes.

Further bending of the nanotube beyond this critical angle results in a series of distortions in the energy curve as indicated by the marks $II-IV$ in Fig. 3. These distortions do not correspond to a formation of a new buckle, but rather to a significant change in the structure of the *two* existing buckles, until a double kink is formed for each buckle. These structural changes involve atoms near the buckle are shown in Figs. 4(c) and 4(d).

The above-outlined procedure, in which a straight nanotube is folded into a closed-ring structure following the adiabatic pathway, was repeated for a series of nanotube lengths and for different nanotube diameters. The adiabatic folding

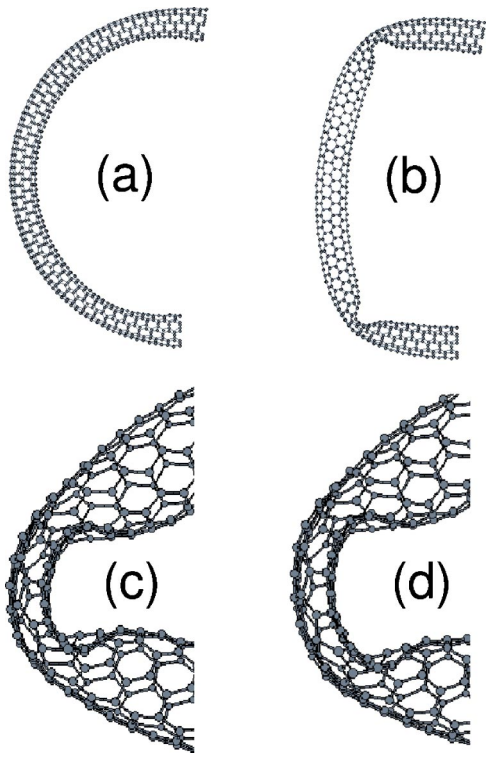

FIG. 4. Buckling of a $5\times5\times45$ nanotube under adiabatic folding. Folding angles are (a) 191°, (b) 191.5°, (c) 348.5°, and (d) 349°.

results *always* in formation of only two buckles below a critical tube length, independent of the nanotube diameter. However, the critical angle at which the kinks are formed does depend on the length and diameter of the nanotube. The closed-ring structures obtained from the adiabatic folding for three nanotubes are shown in Fig. 5. Common to all configurations shown which form buckles (and to others not shown) is that large portions of the folded nanotube resemble a slightly bent nanotube, and most of the tension contributing to higher energies is located in two, well-defined, buckle regions. We refer to this structure as a ''lipslike'' structure for obvious reasons.

The longest nanotube shown in Fig. 5, namely, the $5\times5\times180$ nanotube, does not form a lipslike structure, but rather the adiabatic folding results in a perfect ring. This was also the case when a geometric construction followed by the CG minimization procedure was applied to this nanotube. This result is significant for two reasons: (i) The fact that two

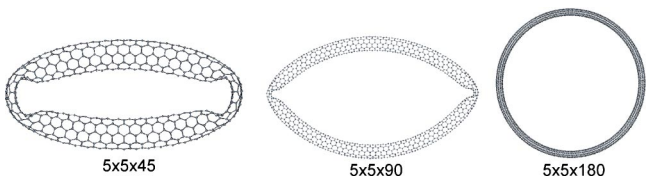

FIG. 5. Results of the total adiabatic folding of $5\times5\times45$, $5\times5\times90$, and $5\times5\times180$ nanotubes. The $5\times5\times180$ forms a perfect ring structure. This result was also obtained using the geometric construction.

different procedures that yield different configurations for shorter nanotubes result in the same final configurations indicates that this indeed is the most stable structure for the $5\times5\times180$. (ii) There is a critical length at which the nanotube does not buckle, and the stable configuration corresponds to a perfect ring structure. This critical length will vary depending on the diameter of the nanotube. As the diameter of the nanotube increases we find that the critical length for the formation of a perfect ring structure also increases.

As will be discussed below, the structure containing only two buckles is more stable than the polygonal structures studied in the previous subsection. The reason is related to the difference between the energy required to form an additional buckle compared to the energy required to further bend an existing buckle, and to form a double-kink buckle. The fact that the two-buckle structure is more stable than the one with many buckles indicates that the energy required to further bend an existing buckle is smaller than the energy required to form an additional buckle. This observation is in agreement with the results shown in Fig. 3, where the energy to form the first two buckles is slightly larger than that required to further bend the buckles to form a double-kink structure.

Despite the fact that these lipslike structures, as will be demonstrated below, are more stable than the polygonal structures, we do not expect that the continuum elastic shell model will provide a qualitative description of the properties of these configurations. The main reason is related to the fact that the energy required to form a double-kink structure is significantly higher than the energy regime at which an elastic behavior is expected.

IV. STABILITY

In this section we discuss the kinetic stability of the structures studied in Sec. III. Several techniques were used to examine the kinetic stability. First, MC simulations were performed at low and high temperatures. Since the closed-ring structures were found to be stable during the entire simulation run, we used the NEB method to calculate the energy barriers for transition between the different structures. In addition, we have also used the NEB method to study the breakage of a closed-ring structure into the corresponding nanotube. All simulations were carried out with the modified Tersoff-Brenner potential. We note in passing that a version of this potential has also been applied to study unimolecular dissociation of alkane chains, with remarkable success in predicting the dissociation rates, and thus the activation barriers.[28]

The large energy associated with the buckles formed when a nanotube is folded into a closed-ring structure may lead one to assume that these structures are unstable kinetically, and will break spontaneously even at low temperatures. Obviously, these structures are less stable thermodynamically compared to the corresponding nanotube, however, their kinetic stability is an open problem.

Given these facts we have carried out MC simulations to study the stability of these structures on microscopic time scales. The simulations were carried out at high temperatures in order to accelerate any conformational change, if they occur. Simulations of these materials at high temperature are possible since the carbon-carbon bond is extremely strong, and dissociation occurs only at very high temperatures.

First, we studied the stability of the polygonal structures, which were found to be stable during the entire simulation time for temperatures as high as 2000 K. At 4000 K bonds begin to break, and at temperatures higher than 5000 K the close-ring structure collapses. Similar results were obtained from MD runs under similar conditions. The MC runs below 2000 K indicate that the initial polygonal structure is stable during the entire simulation, and we do not observe conformational changes to other polygonal structures. The simulations do show that local deformations occur at temperatures below 2000 K. However, these typically relax back into the initial polygonal structure. These defects were not observed at room temperature (300 K) on the time scale of the simulations. The structural changes observed above 2000 K and before the closed-ring collapses are mainly related to transitions of the polygon into a ring. Namely, the buckling of the nanoring disappears.

A similar analysis was carried for the lipslike structures generated by adiabatically folding the nanotube into a closed-ring structure, as described in Sec. III. At temperatures below 2000 K the lipslike structure is stable during the entire run, similar to the case of polygonal structures. Differences were observed at relatively high temperatures, above 2000 K, where heptagon-pentagon defects were formed at the buckles. Above 3000 K the lipslike structure is unstable even on the short time scale of the simulations. This instability results in bond breakage, and the lipslike structure becomes somewhat disordered.

The MC simulations indicate that the lipslike and polygonal structures are stable even at fairly high temperatures during the entire simulation runs. Surprisingly, the high energy associated with the buckling of the nanotube does not result in breakage when the temperature is relatively high (2000 K). Furthermore, on the time scale of the computer simulations no structural transformation between different polygonal structures was observed, indicating that the time scales for such processes are fairly long.

Since the MC and MD simulations are restricted to relatively short time scales, we have adopted the NEB method[25–27] to study the minimum-energy path (MEP) between different polygonal structures in order to address the issue of their kinetic stability. Specifically, we have applied the NEB method to study the MEP between the lipslike and the polygonal structures obtained using the two different construction paths described in Sec. III. In addition we have studied the minimum energy required to open these closed-ring structures into the corresponding nanotubes.

In Fig. 6 we show the minimum-energy path obtained using the NEB method where the initial and final configurations were the lipslike and polygonal structures, respectively. Eleven images were used to construct the path. As clearly can be seen in the figure, the lipslike structure is far more stable than the corresponding polygonal structure. This was also observed for other closed-ring tubes with different tube diameters and lengths, however, the difference between the

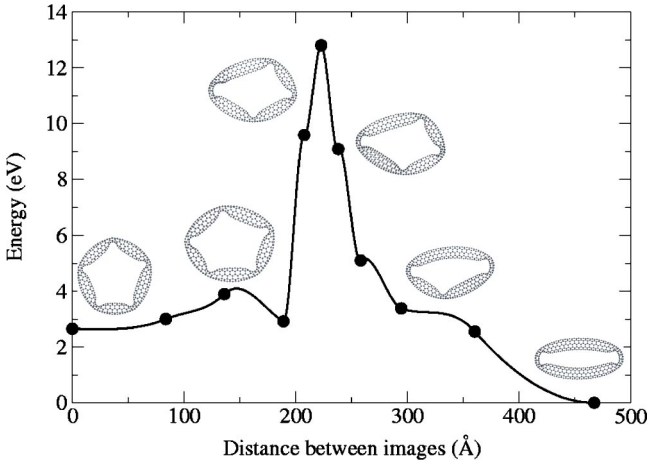

FIG. 6. Minimum-energy path for the internal conversion between a polygonal structure obtained from the geometrical construction and the lipslike structure obtained from folding a carbon nanotube onto itself. The results are for a $5\times5\times45$ structure.

energies of the two configurations decreases with increasing tube length. The minimum-energy path between the two closed-ring structures indicates that upon each formation of an additional buckle, there is an increase in the total energy. The increase in the total energy is somewhat compensated by the release of energy from the double kinks in the lipslike structure. The structure of the closed-ring tube at the transition state is characterized by four buckles. The activation energy for this conformational change is approximately 10 eV. The formation of the fifth buckle which gives the structure of the relaxed polygon results in a reduction of the energy of the closed ring. An additional energy gain is achieved when the squashed five-apex polygon structure is further relaxed to the final polygonal structure. This final relaxation is obviously not the bottleneck for this conformational change.

The major conclusion drawn from this simulation is that the barrier height for the lips-to-polygon conformational transformation is very high, much higher than the thermal energy at room temperature. Even at very high temperatures, the transformation between the two structures is unlikely to happen. What will happen is that the more stable lipslike structure will dissociate before a conformational transformation occurs.

Much higher barriers were observed when the polygonal structure undergoes a unimolecular dissociation into the corresponding nanotube. The most significant contribution to the barrier height corresponds to the breakage of carbon-carbon bonds at the cross section of the nanopolygon. Only after these bonds break is there a significant energy gain when the kinks open up, and the polygon relaxes into the final tube structure. Though energetically unfavorable with respect to the nanotube structure, once created, the closed-ring structures are expected to have long-term stability.

V. CONCLUSIONS

In this work we have discussed the structural properties of a class of closed-ring carbon nanotubes. First, we extended the elastic shell model of Yakobson *et al.*[12] to treat the case of multi-, uncorrelated, buckle formations. The model provides a relation between the length and diameter of the tube to the resulting closed-ring structure. Specifically, it predicts that the number of apexes increases with the square root of the length of the tube (L) and decreases with the square root of the diameter of the tube (d).

To assess the accuracy of the elastic shell model we have performed simulations using the modified Brenner potential. Two different pathways were taken to construct the closed-ring structures: the geometric construction and the adiabatic folding. The structures obtained using the adiabatic folding were found to be more stable than those obtained using the geometric construction. These lipslike structures have only two buckles each characterized by a double kink. Given that the energy of the double kink is much higher than the energy regime at which an elastic behavior is expected, it is not surprising that the elastic model fails to predict the minimum-energy structure of the closed-ring configurations.

The large energy associated with the buckles formed when a nanotube is folded into a lipslike structure may lead one to assume that these structures are unstable kinetically. However, MC and MD simulations indicate that on the microscopic time scales of the simulations, the closed-ring structures are very stable, and dissociate only at very high temperatures. Nudged elastic band calculations indicate that the barrier for conformational changes is relatively high, and these closed-ring structures are expected to dissociate before they undergo structural transformations.

ACKNOWLEDGMENTS

This research was supported by Israel Science Foundation founded by the Israel Academy of Sciences and Humanities (Grant Nos. 34/00 and 9048/00). E.R. would like to acknowledge the Israeli Council of Higher Education for the Alon fellowship.

[1] S. Iijima, Nature (London) **354**, 56 (1991).
[2] M. S. Dresselhaus, G. Dresselhaus, and P. C. Eklund, *Science of Fullerenes and Carbon Nanotubes* (Academic, San Diego, 1996).
[3] M. Bockrath *et al.*, Science (Washington, DC, U.S.) **275**, 1922 (1997).
[4] P. G. Collins *et al.*, Science (Washington, DC, U.S.) **278**, 100 (1997).
[5] S. J. Tans, A. R. M. Verschueren, and C. Dekker, Nature (London) **393**, 49 (1998).
[6] R. Martel *et al.*, Appl. Phys. Lett. **73**, 2447 (1998).
[7] M. Menon and D. Srivastava, J. Mater. Res. **13**, 2357 (1998).
[8] S. Ihara, S. Itoh, and J. I. Kitakami, Phys. Rev. B **48**, 5643 (1993).
[9] S. Itoh and S. Ihara, Phys. Rev. B **49**, 13 970 (1994).

[10] S. Ihara and S. Itoh, Carbon **33**, 931 (1995).
[11] S. Iijima, C. J. Brabec, A. Maiti, and J. Bernholc, J. Chem. Phys. **104**, 2089 (1996).
[12] B. I. Yakobson, C. J. Brabec, and J. Bernholc, Phys. Rev. Lett. **76**, 2511 (1996).
[13] D. Srivastava, M. Menon, and K. Cho, Phys. Rev. Lett. **83**, 2973 (1999).
[14] L. Liu, C. S. Jayanthi, and S. Y. Wu, Phys. Rev. B **64**, 033412 (2001).
[15] A. Bezryadin, A. R. M. Verschueren, S. J. Tans, and C. Dekker, Phys. Rev. Lett. **80**, 4036 (1998).
[16] V. H. Crespi, M. L. Cohen, and A. Rubio, Phys. Rev. Lett. **79**, 2093 (1997).
[17] M. B. Nardelli, B. I. Yakobson, and J. Bernholc, Phys. Rev. Lett. **81**, 4656 (1998).
[18] A. Rochefort, P. Avouris, F. Lesage, and D. R. Salahub, Phys. Rev. B **60**, 13 824 (1999).
[19] L. Liu *et al.*, Phys. Rev. Lett. **84**, 4950 (2000).
[20] T. W. Tombler *et al.*, Nature (London) **405**, 769 (2000).
[21] M. B. Nardelli, Phys. Rev. B **60**, 7828 (1999).
[22] J. R. Wood and H. D. Wagner, Appl. Phys. Lett. **76**, 2883 (2000).
[23] V. Meunier, P. Lambin, and A. A. Lucas, Phys. Rev. B **57**, 14 886 (1998).
[24] D. W. Brenner, Phys. Rev. B **42**, 9458 (1990).
[25] H. Jonsson, G. Mills, and K. W. Jacobsen, *Nudged Elastic Band Method for Finding Minimum Energy Paths of Transitions in Classical and Quantum Dynamics in Condensed Phase Simulations* (World Scientific, Singapore, 1998).
[26] G. Henkelman, B. P. Uberuaga, and H. Jonsson, J. Chem. Phys. **113**, 9901 (2000).
[27] G. Henkelman and H. Jonsson, J. Chem. Phys. **113**, 9978 (2000).
[28] S. J. Stuart, B. M. Dickson, D. W. Noid, and B. G. Sumpter (unpublished).